

Computational Study for Axisymmetric Nozzle at Transonic and Supersonic Flow Regime

Berker Özkaraduman

Turkish Aerospace

Ankara, Turkey

berker.ozkaraduman@gmail.com

Abstract

Computational Fluid Dynamics (CFD) analyses of axisymmetric circular-arc boattail nozzle geometry are performed in this study to investigate both external and internal flow field around nozzle for transonic and supersonic flow regimes. Commercial (ANSYS Fluent) and open source softwares (SU2) are employed. Then, they are compared with experimental data. Analyses are performed at freestream Mach numbers of 0.9 and 1.2. Nozzle pressure ratios (NPR) of 4 and 6 are used at freestream Mach number of 0.9 and 1.2. 2D and 3D grids are employed. SST turbulence models in both solvers yield the best overall agreement with the experimental data.

1. Introduction

Computational Fluid Dynamics (CFD) analyses of an axisymmetric convergent-divergent nozzle at transonic and supersonic freestream conditions have been carried out to test Reynolds-Averaged-Navier-Stokes (RANS) turbulence models of ANSYS Fluent and SU2. CFD runs are validated with experiment which has been performed for axisymmetric nozzle [1]. Experimental setup can be investigated from Figure 1. Experiment includes five nozzle configurations which are given in Figure 2. "Configuration 2" is selected for validation. Computations has been made at both transonic and supersonic flow regions with different NPR's (Nozzle Pressure Ratio). At these NPR's, flow exhibits shock waves, shear layer and shock induced separation which are challenging for flow modeling. Owing to advances in fidelity level of CFD, it is aimed to have better approach for nozzle performance, nozzle design, nozzle drag, after body drag etc.

Similar studies have been performed in the past. Wind code has been tested by using "Configuration 2" [2]. Both transonic and supersonic freestream conditions are used with NPR of 4 and 6 [2]. In particular, 2D, axisymmetric analysis was performed. Several turbulence models were tested and it was found the fact that SST denotes the best overall agreement with experimental data [2]. Moreover, similar study has been performed with same geometry [3]. However, numerical predictions have been completed at Mach 0.9 and NPRs of 4, 5 and 6 with PAB3D CFD code [3]. Also, CFD analysis via Pressure Based Coupled Solver of ANSYS Fluent has been performed by using "Configuration 2" [4]. Analyses are performed at Mach 0.6, 0.9 and 1.2 and NPR of 6. In addition, analysis on SU2 has been performed by validating experiment of Acoustic Reference Research 2 (ARN2) nozzle [5]. It is different from previous studies since they are based on [1]. Turbulent round jets are investigated with SU2 [5].

Since there are 2 types of analysis 2D, and 3D, they are discussed in different sections. Aim is to get results for 3D analysis which makes 2D analysis as a step.

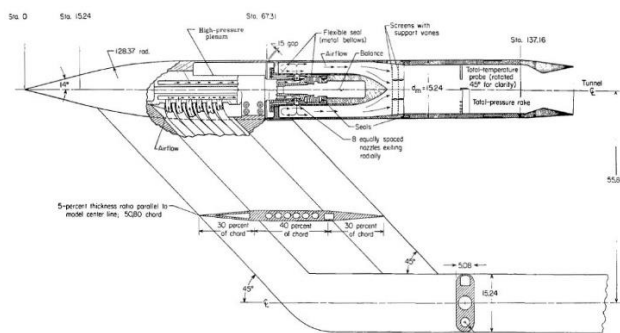


Figure 1 Experimental Setup of [1]

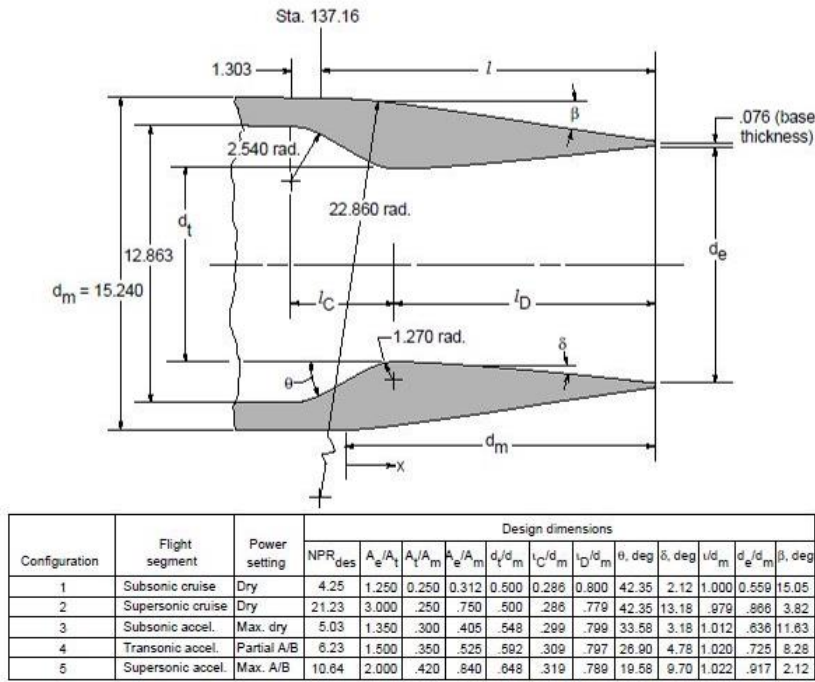


Figure 2 Details of Nozzle Configurations Used in [2] and [3] and Technical Drawing of "Configuration 2" (Adopted from [3])

2. Cases

Analyses are performed in ANSYS Fluent and SU2. ANSYS Fluent version of 17 is used; while, Blackbird 7.1.0 version of SU2 is used. Then, results are compared with experiment [1]. For the external pressure distribution, Cp curves are produced. Moreover, for the internal surface pressure, p_s/p_t curves are produced in order to compare CFD results with experimental data. Cp is defined as

$$C_p = \frac{P_s - P_\infty}{q_\infty} \quad (1)$$

where P_s : surface pressure, P_∞ : ambient pressure and q_∞ : ambient dynamic pressure. All freestream parameters are inputs of boundary conditions. Only P_s is extracted from analysis. For the internal surface pressure, p_t is total pressure of nozzle inflow (total pressure of gas in nozzle); while, p_s is extracted from analysis which is static pressure of nozzle surface.

2.1 Turbulence Modeling

For 2D and 3D analysis density based solver is employed in SU2. However, density based solver is employed in 2D analysis in ANSYS Fluent; while, pressure based solver is employed in 3D analysis in ANSYS Fluent.

For density based solver, the continuity and momentum equations are solved simultaneously. Pressure field is extracted from equation of state. In addition, the density field is extracted from the continuity equation. Owing to these, accurate representation of shocks and acute flow gradients (seen in boundary layer and shear layers) are resolved. However, pressure based solver works differently. The pressure field is outcome of pressure or pressure correction equation which is extracted from manipulation of continuity and momentum equation.

For both 2D and 3D analysis RANS turbulence models are employed. Since case includes separation at internal nozzle surface, no wall functions are utilized. Spalart Allmaras (SA) and Shear Stress Transport (SST) models are used. Both are them Low Reynolds turbulence model which implies y^+ value should be closer to 1 in order to capture boundary layer's dramatic velocity gradient behavior. SA employs one transport equation to model the turbulent viscosity which is also called the kinematic eddy viscosity. SST is 2 equation eddy viscosity turbulence model which is hybrid combination of Wilcox $k-\omega$ and $k-\epsilon$ model [6]. k is the turbulent kinetic energy; while, ω the specific dissipation rate which is obtained dividing the turbulent dissipation rate (ϵ) by the turbulent kinetic energy (k). Moreover, $k-\epsilon$ realizable turbulence model which is high Reynolds turbulence model is employed with enhanced wall treatment for 3D analysis in ANSYS Fluent. According to ANSYS Fluent's user guide, in $k-\epsilon$ realizable turbulence model, the turbulent viscosity

has an alternative formulation and the turbulent dissipation rate is derived from an exact equation for the transport of the mean-square vorticity fluctuation.

2.2 2D Analysis

Both commercial and open source softwares are to be tested.

2.2.1 Numerical Model

Density based solvers are used. Flow is assumed axisymmetric and steady. Sutherland Law of viscosity with 3 coefficient is used. Air is modeled as perfect gas. Walls are assumed to be adiabatic. Roe flux scheme is utilized. 2nd order upwind scheme is used in ANSYS Fluent. However, MUSCL_FLOW (Both in SA and SST) and MUSCL_TURB (only in SST) schemes are activated in SU2 analysis. Green Gauss Node Based is selected or gradient scheme. Both Spalart Allmaras (SA) and Shear Stress Transport (SST) turbulence models are employed in two softwares. For ANSYS Fluent analysis, Courant number (CFL-Courant-Friedrichs-Lewy) of 1 is started and increased step by step to 5 in 50 000 iterations. While, adaptive CFL number from 1 to 20 is employed for SU2 analysis in 50 000 iterations.

2.2.2 Mesh Details

Computational domain extends 1600 nozzle outside diameters downstream and 200 nozzle outside diameters to upstream. It extends 227 nozzle outside diameters vertically (y axis). Due to the fact that pressure far field boundary condition is employed, domain has large dimensions.

Boundary types used in analysis can be examined from Figure 3. Pressure far field region is given with black color in Figure 3. Axis is given with green line in Figure 3. Adiabatic wall is given with blue line color in Figure 3. For ANSYS Fluent, pressure inlet boundary type is used for nozzle inflow; while, supersonic inlet boundary type is employed in SU2 for nozzle inflow. Domain and boundary types can be inspected from Figure 3.

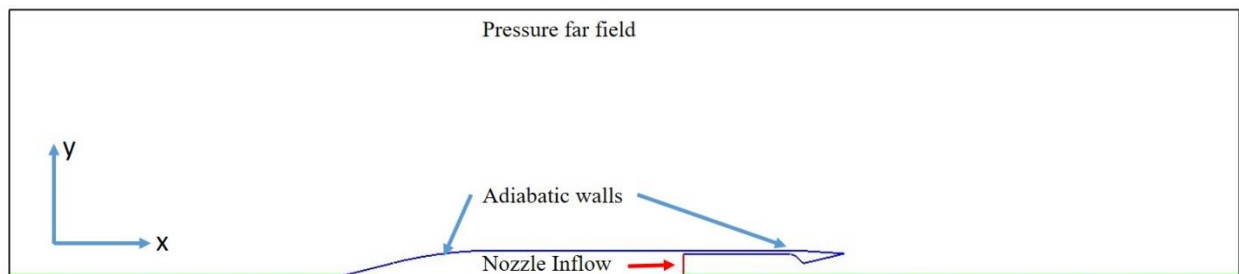


Figure 3 Domain and Boundary types for 2D Analysis

Mesh was built in ANSYS Mesher. Structured mesh is usually preferred in jet exhaust problems. Nevertheless, creation of structured mesh brings excessive element count for complex geometries. In addition, up to date solvers are capable of managing unstructured mesh. For this reason, unstructured mesh is preferred. Therefore, unstructured mesh is created and used for 2D analysis. Mesh can be examined from Figure 4. y^+ value of 1 is aimed during mesh generation.

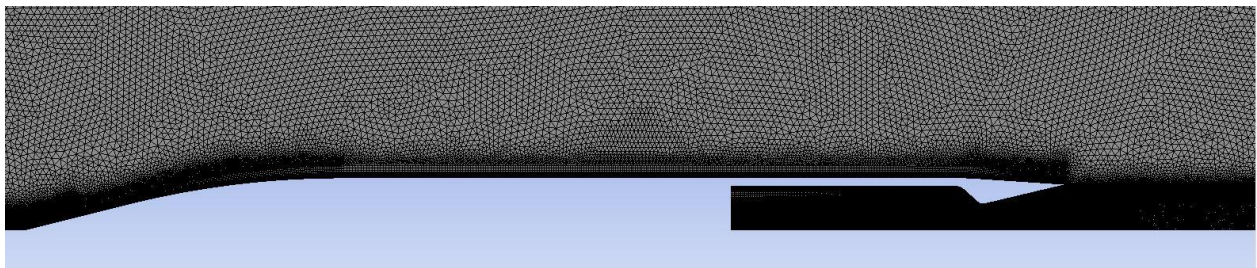


Figure 4 2D unstructured mesh

Due to usage of density-based solver, finer mesh is created at nozzle region. This can be investigated in Figure 5. Since axisymmetric analysis is to be run, half of geometry is meshed. This arises a problem in assigning prism layer. That is, creating prism layer induces poor elements at nose region. Because nose region includes complex physics (shock waves, compression waves etc.), quality of mesh is critical at here. If prism layer is restricted to nose, mesh quality becomes poor. Due to this reason prism layer is extended to front side of nose region. This can be examined in Figure 6. Poor elements can be investigated at bottom left of Figure 6. It is considered that poor elements are acceptable at this region since no complex features in flow field (shock waves, shear layer, boundary layer etc.) occurs at this region. Zoomed view of nose region can be observed in Figure 7. Mesh details are shown in Table 1.

Table 1 2D unstructured mesh details

Number of Elements	407 096
Average Skewness	3.9835e-2
Maximum Skewness	0.9992
Minimum Skewness	0

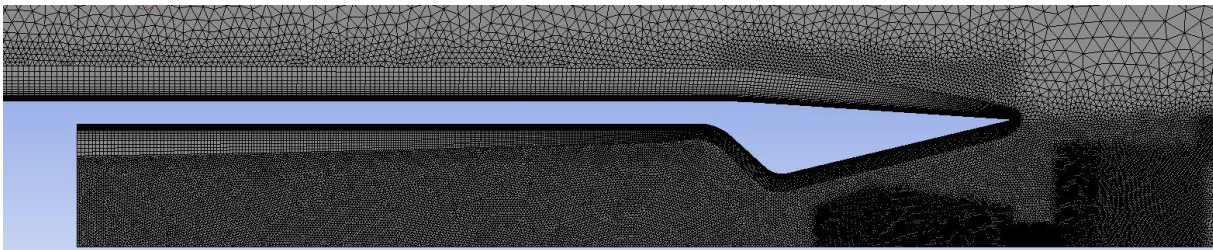


Figure 5 Nozzle region of 2D Mesh

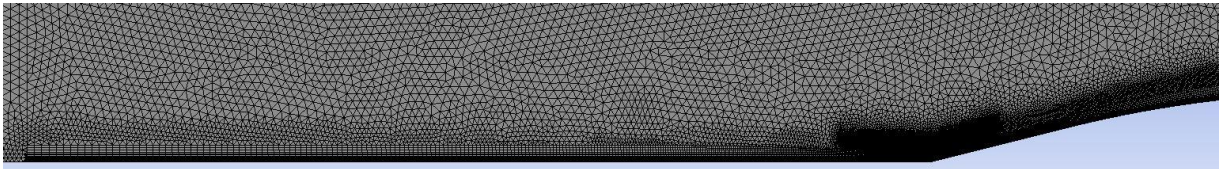


Figure 6 Nose region of 2D Mesh

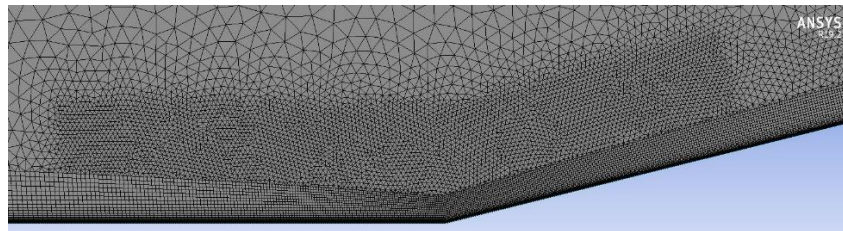


Figure 7 Zoomed view of nose region of 2D Mesh

Boundary conditions are extracted from [2] by using isentropic gas relations.

2.2.4 Mach 0.9, NPR 6

For inputs of boundary conditions, temperature values are in Kelvins; while, pressure values are in Pascals. For the transonic analysis, freestream Mach number of 0.9 with NPR value of 6 case is selected. This case is selected for the reason that separation is delayed so turbulent structures and adverse pressure gradient does not create problematic iterations in solution. Boundary conditions are extracted from [2] by using isentropic gas relations. Boundary conditions defined in CFD analysis are tabulated in Table 2. Velocity_x stands for x component of velocity which is given in Table 2. No other component of velocity (y,z) is given in boundary condition of nozzle inflow for SU2. For both solvers Freestream boundary condition is applied. Nozzle Inflow (Pressure Inlet) is employed for ANSYS Fluent's boundary condition; while, Nozzle Inflow (Supersonic Inlet) is employed for SU2's boundary condition.

Table 2 Boundary Conditions used in 2D Analysis at Mach 0.9, NPR 6

	Freestream (pressure far field)	Nozzle Inflow (Pressure Inlet)	Nozzle Inflow (Supersonic Inlet)
Mach Number	0.9	-	-
Total Temperature (Kelvin)	-	300	-
Total Pressure (Pascal)	-	359 561.60	-
Static Pressure (Pascal)	59 915.44	349 840	349 840
Static Temperature (Kelvin)	277.09	-	297.66
Freestream Velocity(m/s)	300.4587	-	-
Velocity_x(m/s)	-	-	69.20
	Both	Just in ANSYS Fluent	Just in SU2

According to boundary conditions given in Table 2, ambient pressure (can also be called as back pressure) should be 16.9 kPa (kiloPascal) to have design condition of the nozzle which is NPR of 21.23. However, ambient pressure (back pressure) is 59.9 kPa and exit shock condition occurs about 135 kPa. So nozzle operates at overexpansion flow regime. Since exit pressure at the nozzle is different from ambient pressure (back pressure), the jet of gas must be compressed which includes oblique shock waves attached to the exit of the nozzle.

In order to show comparison of results, Mach contours are visualized. By examining Mach contours, general idea about flow could be obtained. That is, these figures can be used to give idea about Mach trend and range. However, these figures should not be used to compare CFD analysis and experimental data directly. Comparisons related with pressure distributions are used to prove fidelity level of CFD analysis. Mach contours extracted from ANSYS Fluent's analysis can be investigated in Figure 8. Likewise, Mach contours extracted from SU2 analysis can be examined in Figure 9. According to previous paragraph, oblique shock waves should be present to adjust nozzle exit pressure making same with ambient pressure. As illustrated in Figure 8 and Figure 9, abrupt change of red contour to green contour at the end of the nozzle can be observed. This change can be attributed to oblique shock waves due to the fact that nozzle operates at overexpansion flow regime.

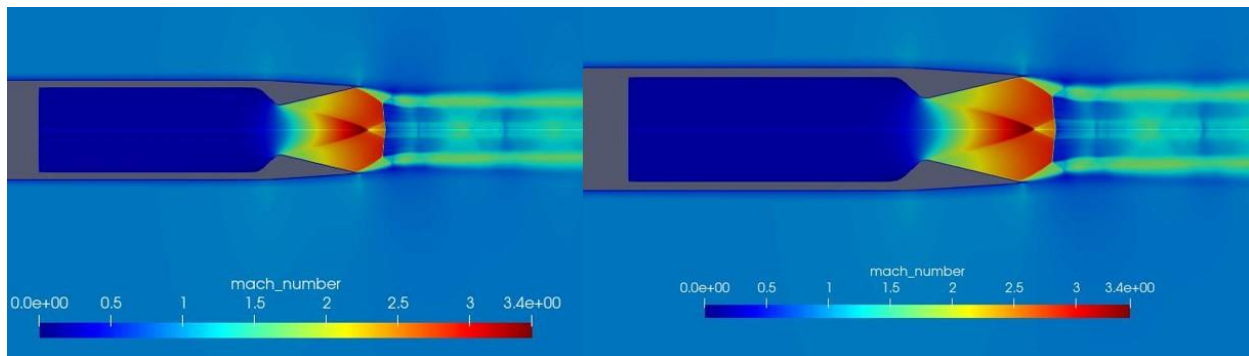


Figure 8 Mach Contours of analysis done with SST and SA models of ANSYS Fluent respectively, for NPR=6, Mach 0.9 case

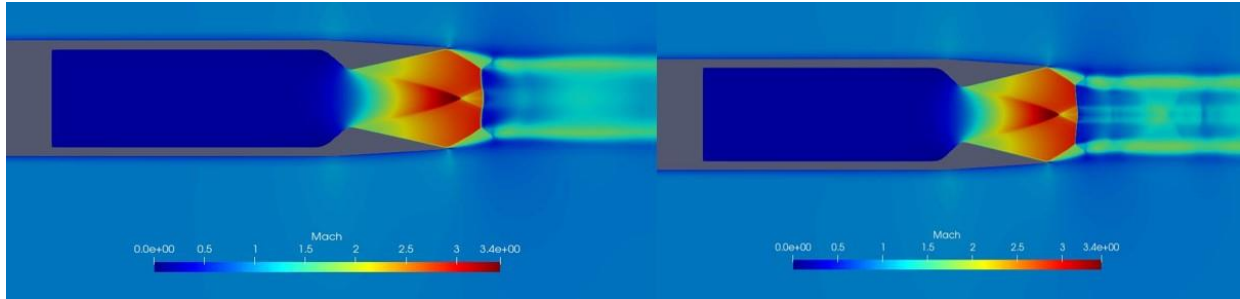


Figure 9 Mach Contours of analysis done with SST and SA models of SU2 respectively, for NPR=6, Mach 0.9 case

The external surface pressure distribution is given in left of Figure 10. Between -0.5 and 0 value of x/D_m , SA turbulence model of SU2 matches exactly with experimental data. However, other turbulence models slightly overshoot experimental data. Between 0 and 0.1 values of x/D_m , pressure values extracted from SU2 are lower than pressure values extracted from ANSYS Fluent. Pressure values extracted from SU2 passes experimental point at this region; while, pressure values extracted from ANSYS Fluent undershoots in this region. After 0.2 value of x/D_m on external surface, all turbulence models of all softwares yield same pressure values. Next, it is sensible to say that all CFD softwares with all turbulence models yield satisfactory pressure distribution on the external surface. The internal nozzle surface pressure distribution is given in right of Figure 10. There is no dramatic difference in internal nozzle surface pressure between ANSYS Fluent and SU2 regardless of turbulence models. All internal nozzle surface pressure distribution matches experimental data in a satisfactory level. All turbulence models of all softwares yields similar separation point which is small region at 0.95 value of x/D_m .

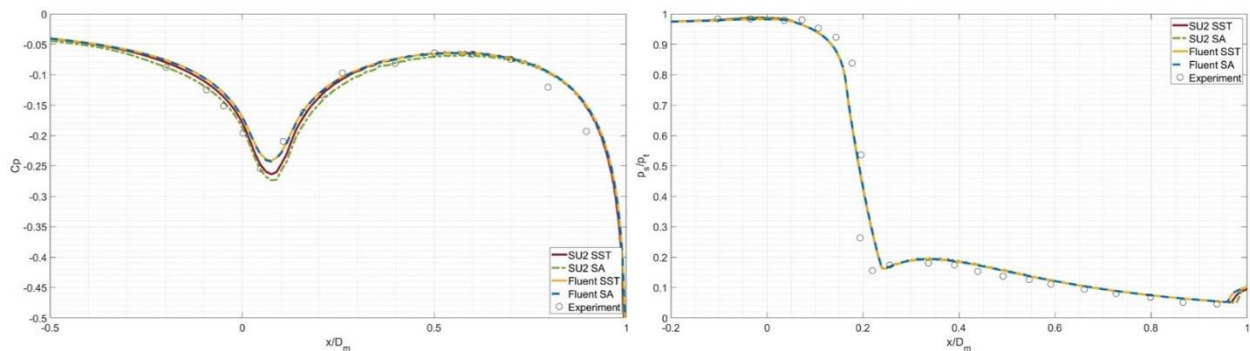


Figure 10 C_p profiles on the external surface and p_s/p_t profiles on the internal nozzle surface at NPR 6 and Mach number of 0.9 ($D_m=15.24$ cm)

2.2.5 Mach 1.2, NPR 4

For the supersonic analysis, freestream Mach number of 1.2 with NPR value of 4 is selected as run case. Boundary conditions are tabulated in Table 3. SA and SST turbulence models of both solvers are compared.

Table 3 Boundary Conditions used in 2D Analysis at Mach 1.2, NPR 4

	Freestream (pressure far field)	Nozzle Inflow (Pressure inlet)	Nozzle Inflow (Supersonic Inlet)
Mach Number	1.2	-	-
Total Temperature (Kelvin)	-	300	-
Total Pressure (Pascal)	-	167 197.9	-
Static Pressure (Pascal)	41 796.02	162 647.3	162 647.3
Static Temperature (Kelvin)	250	-	297.64
Freestream Velocity(m/s)	380.5249	-	-

Velocity_x(m/s)	-	-	69.2
	Both	Just in ANSYS Fluent	Just in SU2

According to boundary conditions given in Table 3, ambient pressure should be 7.87 kPa to have design condition of the nozzle which is NPR of 21.23. However, ambient pressure is 41.8 kPa and exit shock condition occurs about 62.7 kPa. So nozzle operates at overexpansion flow regime. Since exit pressure at the nozzle is different from ambient pressure the jet of gas must be compressed which includes oblique shock waves attached to the exit of the nozzle.

Mach contour extracted from analysis of ANSYS Fluent with k- ω SST turbulence model is given in Figure 11.

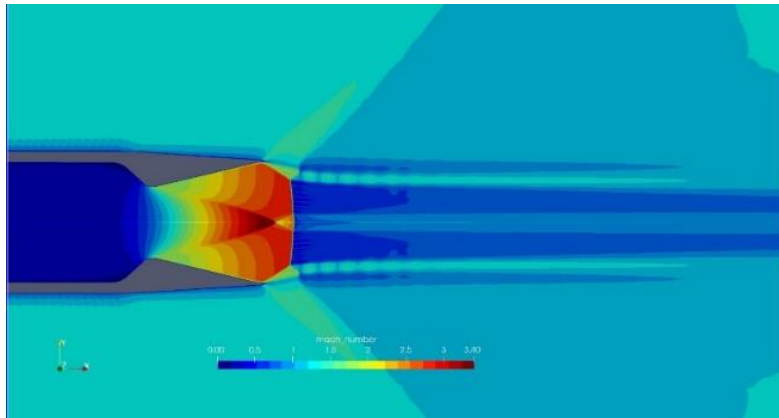


Figure 11 Mach Contours of analysis done with SST turbulence model of ANSYS Fluent respectively, for NPR=4, Mach 1.2 case

Mach contour extracted from analysis of SU2 with SA and SST turbulence models are given in Figure 12.

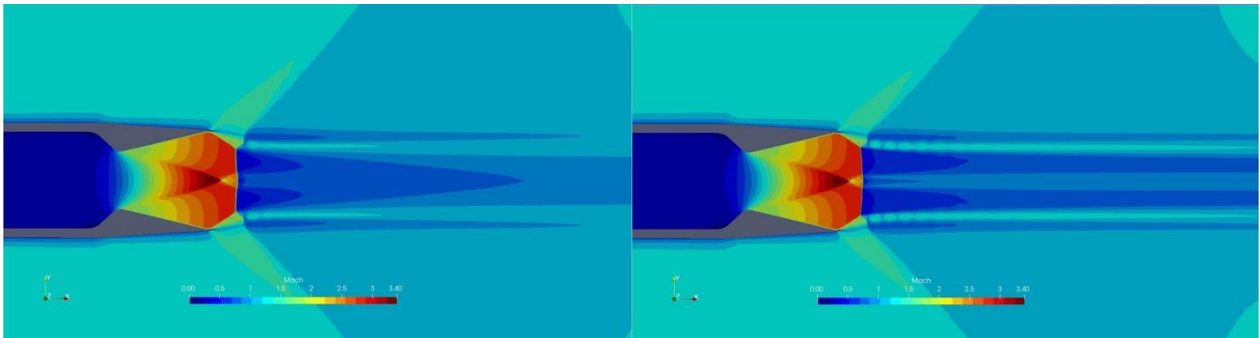


Figure 12 Mach Contours of analysis done with SST and SA models of SU2 respectively, for NPR=4, Mach 1.2 case

Since nozzle operates at overexpansion flow regime, it is foreseen to have oblique shock waves due to compression of gas exiting nozzle. This can be investigated by Figure 11 and Figure 12. As illustrated in Figure 11 and Figure 12, there is an abrupt Mach number change near the wall with oblique shape at the exit of the nozzle.

As illustrated in left of Figure 13, SU2 yields compatible pressure values and trend with respect to experiment. In addition, there is fluctuation of C_p values between 0.1 and 0.4 value of x axis in ANSYS Fluent's result. This is not physically sensible. So, grid independency study is going to be performed at [2.2.6](#) for ANSYS Fluent's density-based solver.

The internal nozzle pressure distribution plots of CFD analysis and experiment are shown in left hand side of Figure 13. As seen in right of Figure 13, CFD analysis match well with experimental data. However, there is a slight difference exists between CFD results and experiment in the interval $x/D_m=0$ to $x/D_m \approx 0.25$. CFD Results undershoots pressure values in this region. Both at choking point and after choking, CFD analysis yields good match with experimental data, which can be seen just before $x/D_m=0.25$. Both softwares yield similar results with different turbulence models.

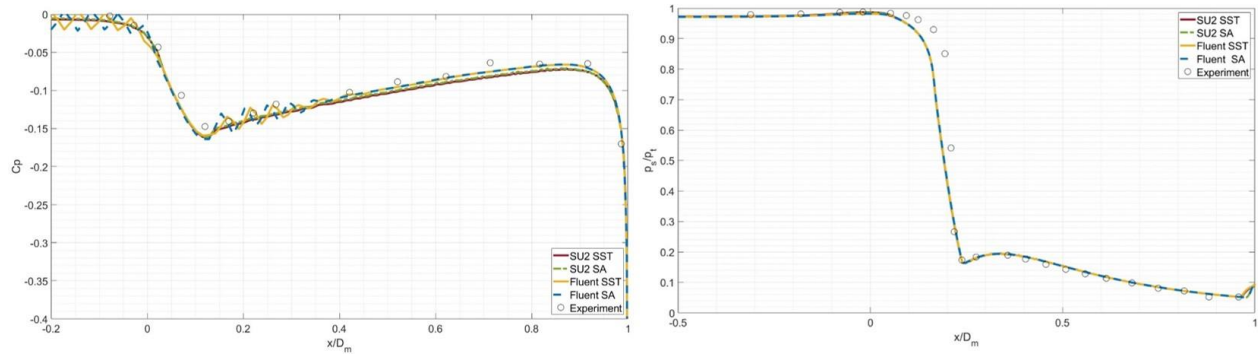


Figure 13 C_p profiles on the external surface and p_s/p_t profiles on the internal nozzle surface at NPR 4 and Mach number 1.2 ($D_m=15.24$ cm)

2.2.6 Grid Independency

Grid independency study is carried out with 4 grids. Details of grids is given in Table 4. Since oscillation occurs at boattail of external surface grid is refined for this region.

Table 4 Grids for 2D geometry

Mesh	Number of Elements
Mesh 1	407 096
Mesh 2	418 054
Mesh 3	434 649
Mesh 4	437 713

Finest mesh which is Mesh 4 is given in Figure 14.

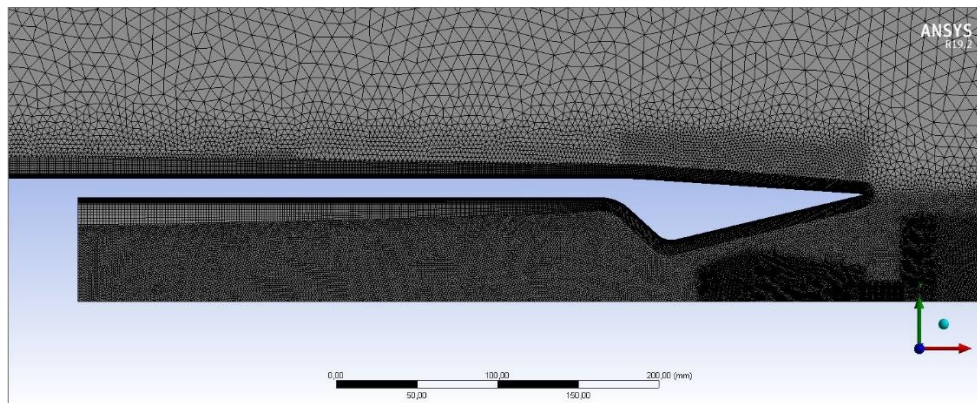


Figure 14 Mesh 4 for 2D grid independency

Since internal nozzle surface p_s/p_t profile is similar in Figure 13, external surface C_p profile is given in Figure 15. Zoomed version of external pressure distribution is given at right hand side of Figure 15. As illustrated Figure 15, the finer mesh become at boattail section the more damped pressure distribution is obtained.

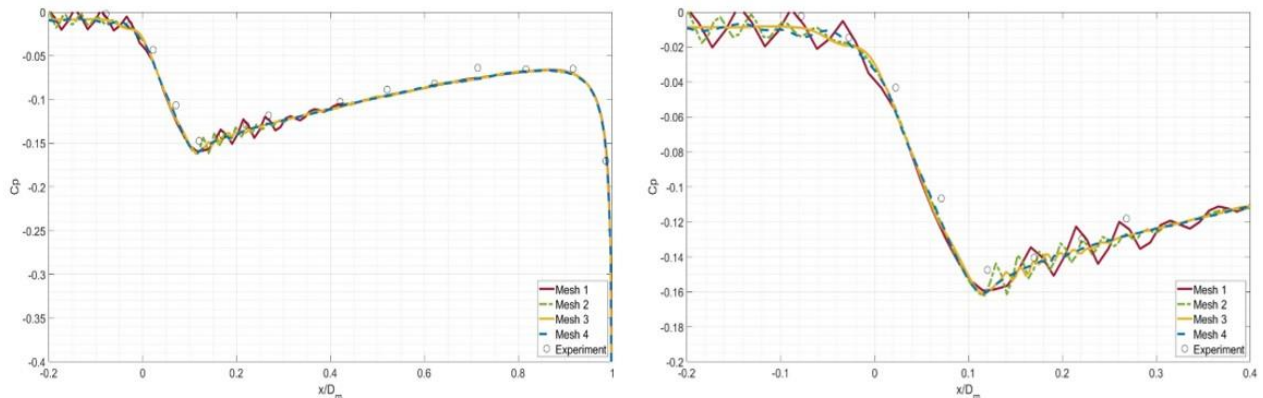


Figure 15 Cp profiles on the external surface at NPR 4 and Mach number 1.2, 2nd figure is zoomed version ($D_m=15.24$ cm)

2.3 3D Full Geometry Analysis

2.3.1 Numerical Model

In this section, analysis is carried out with mainly SU2. ANSYS Fluent's density-based solver cannot be presented due to convergence problems; however, PBCS (Pressure Based Coupled Solver) of ANSYS Fluent's turbulence models are going to be presented— ω SST, SA and $k-\epsilon$ realizable turbulence models are used for ANSYS Fluent's analysis. In addition, two turbulence models (SA, SST) with two schemes (ROE, SST) are to be tested with SU2. Same assumptions and inputs are employed as in 2.2.1 except axisymmetric assumptions. 50 000 iterations are performed for SU2 analysis; while 7100 iterations are done for ANSYS Fluent PBCS solver analysis.

2.3.2 Mesh Details

Computational domain is created cylindrically. Its diameter size is 750 nozzle outside diameters (roughly 100 m). It extends 1500 (roughly 200m) nozzle outside diameters downstream and 580 nozzle outside diameters (roughly 77m) to upstream. Due to the fact that pressure far field boundary condition is employed, domain has large dimensions. Boundary types and section view of domain can be investigated by Figure 16.

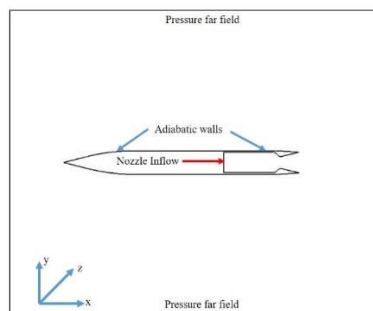


Figure 16 Domain and Boundary types for 3D Analysis

The mesh built in ANSYS Mesher. BOI (Body of Influence) is employed. BOI is used to refine a specific region in the mesh. Mesh is shown in Figure 17. Finer mesh is assigned to the nozzle interior. As seen in the top of Figure 18, there is a finer mesh at the nozzle. Due to the fact that a shock wave occurs at the end of the nozzle, a finer mesh is created in the region where the internal flow encounters and mixes with the external flow. In fact, this region includes the highest gradients in the flow. It can also be investigated in the bottom right of Figure 18. As illustrated in the bottom left of Figure 18, there is a BOI assigned to the nose region. Mesh details can be investigated by Table 5. y^+ value of 1 is aimed during mesh generation.

Table 5 3D unstructured mesh details

Number of Elements	13 739 125
Average Skewness	0.3218
Maximum Skewness	0.9137
Minimum Skewness	2.3716e-5

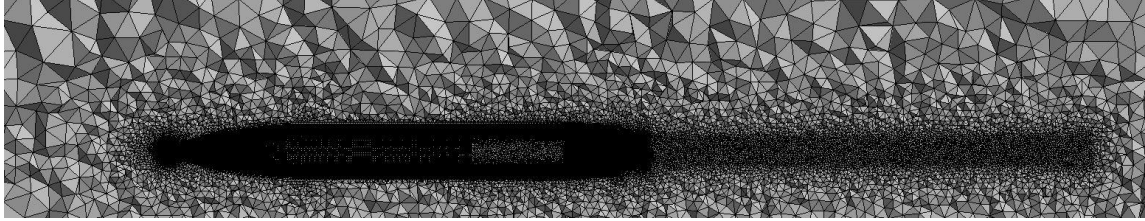


Figure 17 Mesh

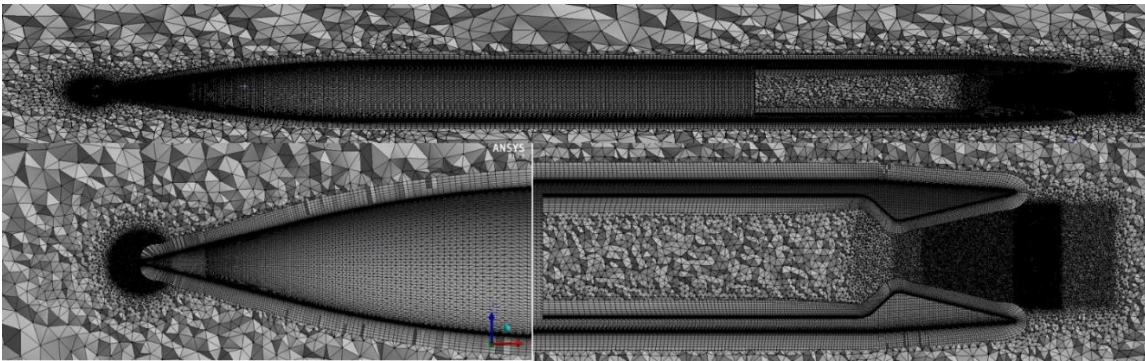


Figure 18 Close View of Mesh Full geometry given in Top View, Nose given at bottom left nozzle region is given bottom right

2.3.4 Mach 0.9, NPR 6

Same boundary conditions are employed with [2.2.4](#).

Mach contours of SU2 are given in Figure 19. At top left corners of Mach contours shown in Figure 19, convective schemes is written first. Then, turbulence models employed for analysis is written. To be compared with [1], similar figure is generated in Figure 19. Turbulence models with different convective schemes predict core flow with minor differences. This can be investigated by nozzle region shown in Figure 19. Also, Mach contour obtained from ANSYS Fluent's PBCS with $k-\omega$ turbulence model is presented in Figure 20. Mach contour of ANSYS Fluent's PBCS with $k-\omega$ turbulence model resembles to Mach contour given by JST SA from SU2 analysis the most. Comment made on [2.2.4](#) about Mach Contours is also valid on this section.

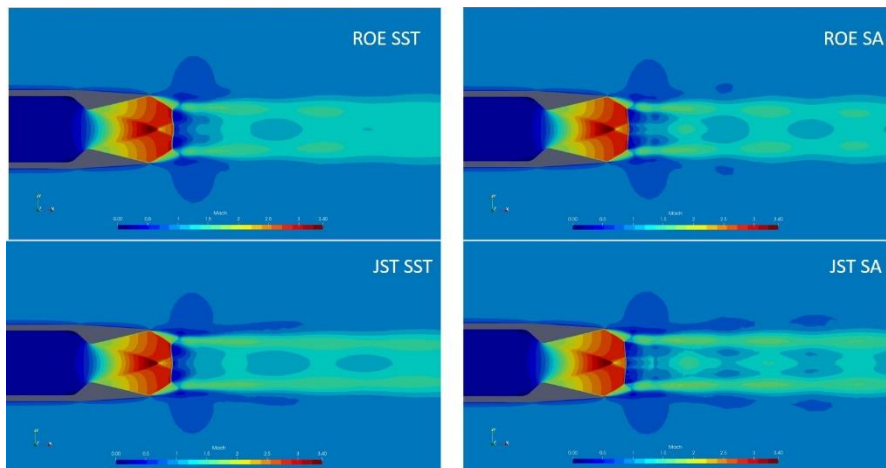


Figure 19 Mach Contours from SU2 Analysis for the NPR=6, Mach 0.9 case

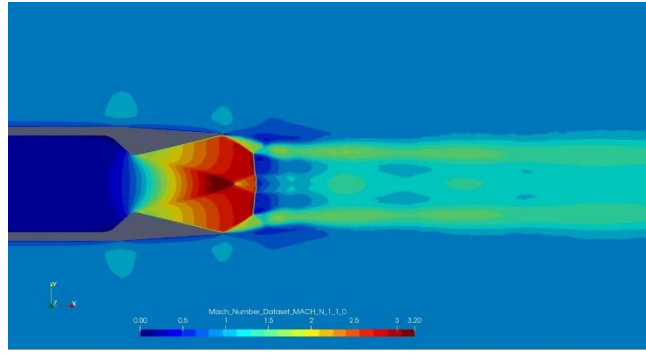


Figure 20 Mach Contour from k- ω SST turbulence model of ANSYS Fluent PBCS analysis for the NPR=6, Mach 0.9 case

External surface C_p profiles and internal nozzle surface p_s/p_t profiles are given in left of Figure 21. As seen in left of, all employed turbulence models in SU2 and SST of ANSYS Fluent PBCS yield similar result for C_p profile on the external surface except k- ϵ realizable and SA turbulence models of ANSYS Fluent. After 0.1 point of x/D_m , pressure values extracted from these turbulence models are slightly different and discrepant from experimental data. All turbulence models yield consistent values and trend with experiment for p_s/p_t profiles on the internal nozzle surface. This can be investigated by right of Figure 21. In summary, there are no distinctive differences on trend with respect to usage of turbulence models with different convective schemes for both C_p profiles and p_s/p_t profiles.

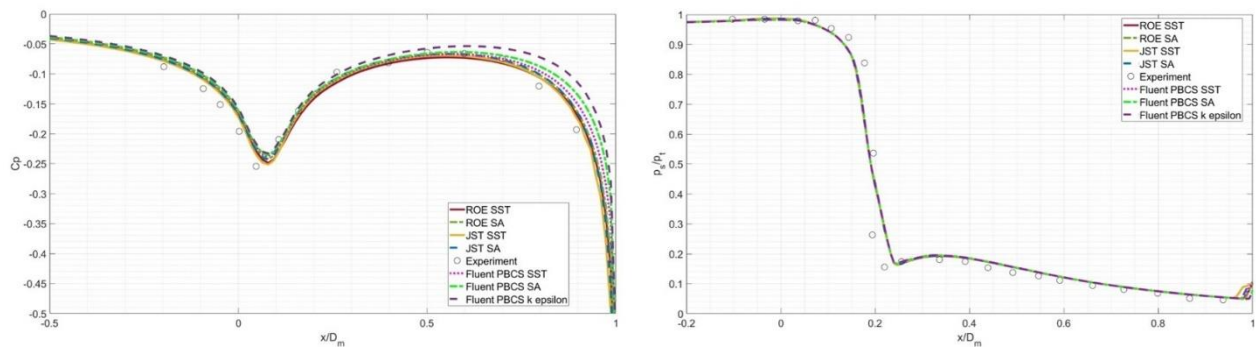


Figure 21 C_p profiles on the external surface and p_s/p_t profiles on the internal nozzle surface at NPR 6 and Mach number 0.9 ($D_m=15.24$ cm)

2.3.5 Mach 0.9, NPR 4

Boundary conditions are given in Table 6.

Table 6 Boundary Conditions used in 2D Analysis at Mach 0.9, NPR 4

	Freestream (pressure far field)	Nozzle Inflow (Pressure inlet)	Nozzle Inflow (Supersonic Inlet)
Mach Number	0.9	-	-
Total Temperature (Kelvin)	-	300	-
Total Pressure (Pascal)	-	239 760.7	-
Static Pressure (Pascal)	59 915.44	223 597	223 597
Static Temperature (Kelvin)	277.09	-	294.09
Freestream Velocity(m/s)	300.4587	-	-
Velocity_x(m/s)	-	-	68.786
	Both	Just in ANSYS Fluent	Just in SU2

According to boundary conditions given in Table 6 , ambient pressure) should be 16.9 kPa to have design condition of the nozzle which is NPR of 21.23. However, ambient pressure (back pressure) is 59.9 kPa and exit shock condition occurs about 134.87 kPa. So nozzle operates at overexpansion flow regime. Since exit pressure at the nozzle is different from ambient pressure the jet of gas must be compressed within oblique shock waves attached to the exit of the nozzle.

Mach contours of SU2 are given in Figure 22, they are similar and acceptable except one selection. As seen from Figure 22, there is numerical instability in Mach contour SA turbulence model with JST convective scheme. So, it could not be reliable. Mach contour obtained from ANSYS Fluent's PBCS is shown in Figure 23. This Mach contour is different from Figure 22 which is the most attractive point the fact that exit shock Mach profile is different. As stated in previous paragraph it is foreseen to have compression of gas exiting the nozzle. This can be investigated by Figure 22 and Figure 23, there is dramatic color change in Mach contours inside the nozzle. Also, this change is closer to throat with respect to other cases which are with 0.9 Mach with NPR 6 and 1.2 Mach with NPR 4.

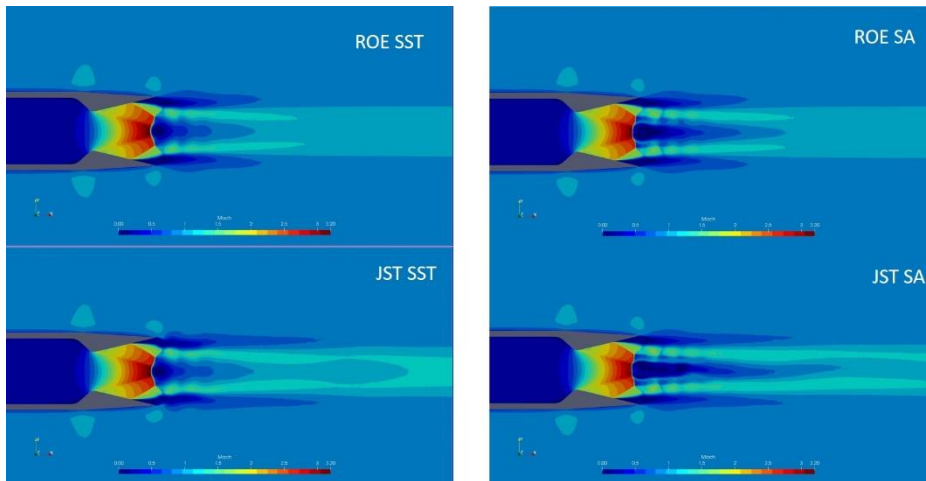


Figure 22 Mach contours obtained from SU2 for the NPR=4, Mach 0.9 case

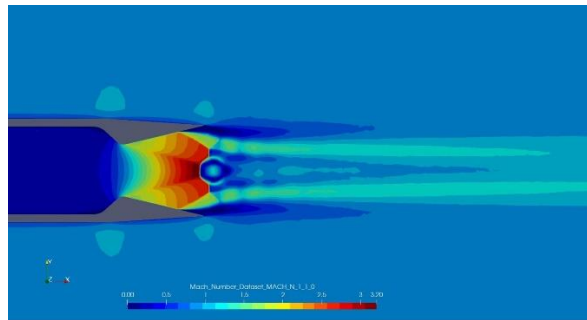


Figure 23 Mach contour obtained from $k-\omega$ SST turbulence model of ANSYS Fluent (PBCS) for the NPR=4, Mach 0.9 case

C_p profile on the external surface is given in left of Figure 24. As seen from 0.07 value of x -axis, turbulence models yield different C_p values regardless of convective schemes for SU2 analysis. SST turbulence yield closer C_p value to experiment at 0.07 value of x -axis. However, all selected turbulence models and schemes yield acceptable external pressure distribution for SU2. There is no remarkable difference in C_p values estimated by $k-\omega$ SST turbulence model of ANSYS Fluent's PBCS at right of Figure 24. After 0.1 point of x/D_m in left of Figure 24, $k-\epsilon$ realizable and SA turbulence model of ANSYS Fluent yield discrepant pressure values with respect to pressure values extracted from SU2 and $k-\omega$ SST turbulence model of ANSYS Fluent.

The internal nozzle surface pressure distribution is illustrated left of Figure 24. On the contrary of previous cases, there are differences. Firstly, there is difference in pressure values which is located between 0.6 and 0.8 value of x/D_m . Zoomed version of plot around this region is given in Figure 25. Between 0.6 and 0.8 value of x/D_m , shock induced separation occurs creating dramatic pressure changes. As seen from right of Figure 25, SST turbulence model with Roe convective scheme in SU2 and $k-\omega$ SST turbulence model in ANSYS Fluent's PBCS yield the closest separation location with respect to experiment. While all turbulence models regardless of convective scheme in SU2 predict early separation, all turbulence models of ANSYS Fluent predict late separation at internal nozzle surface. Roe convective scheme with SST of SU2 and $k-\omega$ SST turbulence model of ANSYS Fluent yield closest separation point with respect

to experiment, according to Figure 25. While JST convective scheme SA turbulence model in SU2 selection yields the earliest separation at internal nozzle surface, A turbulence model of ANSYS Fluent yield the latest separation point at internal nozzle surface. $k-\epsilon$ realizable turbulence model of ANSYS Fluent's PBCS yield the highest pressure value after separation point in internal nozzle surface. This can be investigated right after separation point which is located about 0.73 value of x/D_m by examining right of Figure 24. There is a discrepancy in p_s/p_t values which is located between 0 and 0.2 value of x -axis. This result is similar to 2.2.4 and 2.2.5. This can be examined from right of Figure 24. From 0 to 0.2 values of x -axis $k-\epsilon$ realizable and SA turbulence model ANSYS Fluent's PBCS estimated closer pressure values with respect to experiment which is given in right of Figure 24. To conclude, it can be said that for both softwares SST turbulence model yield the best overall agreement with experiment.

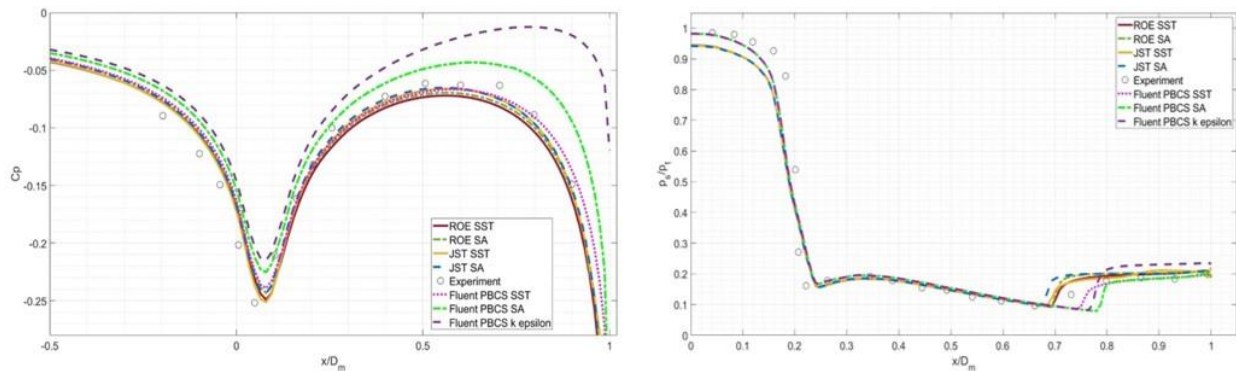


Figure 24 C_p profiles on the external surface and p_s/p_t profiles on the internal nozzle surface at NPR 4 and Mach number 0.9 ($D_m=15.24$ cm)

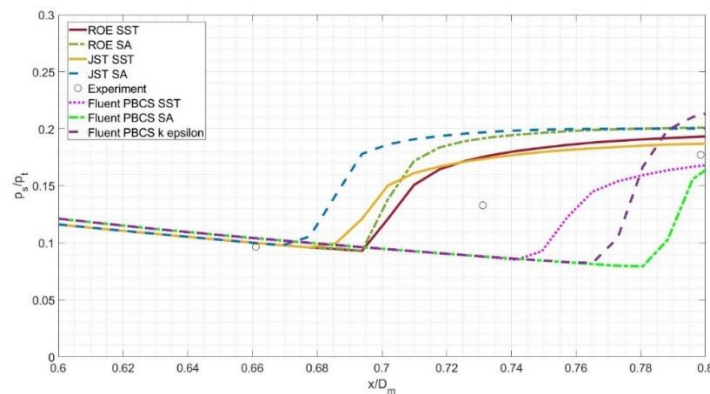


Figure 25 p_s/p_t profiles on the internal nozzle surface at NPR 4 and Mach number 0.9 zoomed of 0.6 and 0.8 values of x/D_m ($D_m=15.24$ cm)

2.3.6 Mach 1.2, NPR 4

Boundary conditions preferred in 2.2.5 is employed for SU2 analysis.

Mach contours obtained from SU2 analysis given in Figure 26. Unlike 2.3.5, there are no numerical instability in Mach contour SA turbulence model with JST convective scheme of SU2. This might be caused by flow regime. In other words, transonic external flow occurs in 2.3.5; while, supersonic external flow occurs in 2.3.6. Therefore, it can be said that numerical stability of supersonic flow regime is higher than stability of transonic regime in SU2. Mach contour obtained from ANSYS Fluent's PBCS is given in Figure 27. This Mach contour is compatible with both Figure 26 and Figure 27. Comment made on 2.2.5 about Mach Contours is also valid on this section.

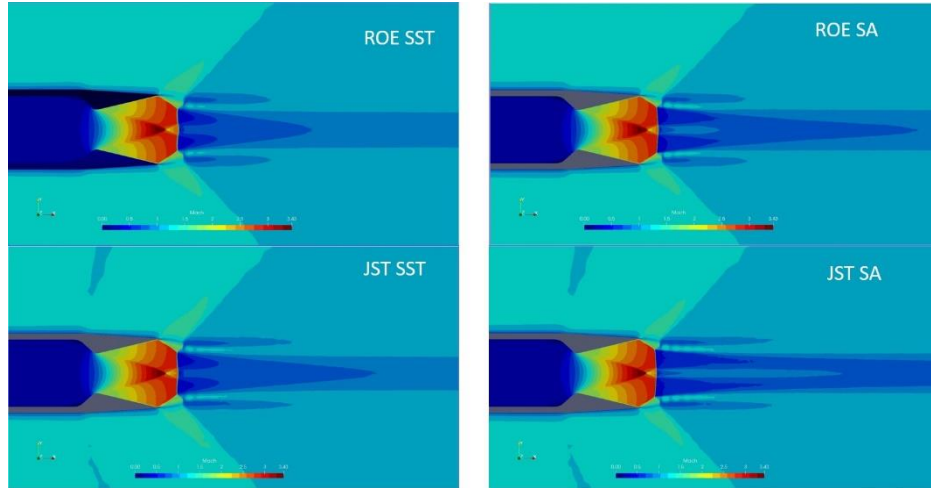
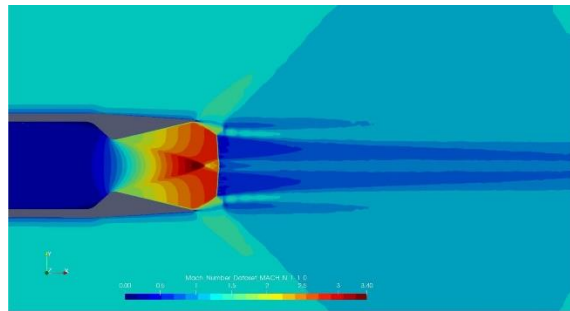
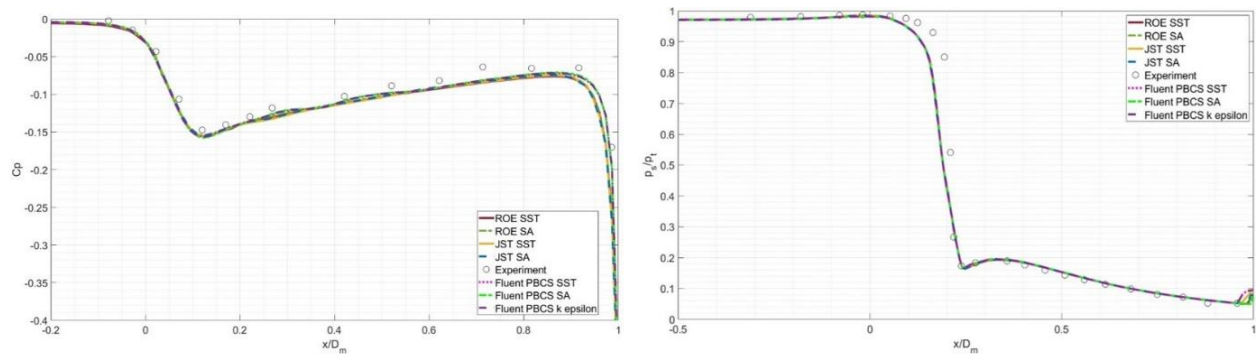


Figure 26 Mach contours obtained from SU2 for the NPR=4, Mach 1.2 case

Figure 27 Mach contours obtained from k- ω SST turbulence model of ANSYS Fluent (PBCS) for the NPR=4, Mach 1.2 case

As seen from left of Figure 28, C_p values and trend extracted from SU2 is compatible with experiment. All turbulence models yield similar C_p values regardless of convective schemes. In addition, C_p profile and trend extracted from ANSYS Fluent's PBCS is compatible with experiment and SU2. However, C_p values extracted from ANSYS Fluent's PBCS includes a slight oscillation between 0.1 and 0.4 value of x-axis. CFD Results extracted from SU2 exhibits smoother behavior with respect to results of ANSYS Fluent's PBCS.

As seen from right of Figure 28, regardless of convective schemes all turbulence models yield acceptable p_s/p_t profiles with respect to experiment. There are no early separation points unlike [2.3.5](#). p_s/p_t profile obtained from ANSYS Fluent's PBCS is given in right of Figure 28. It is compatible with experiment and SU2.

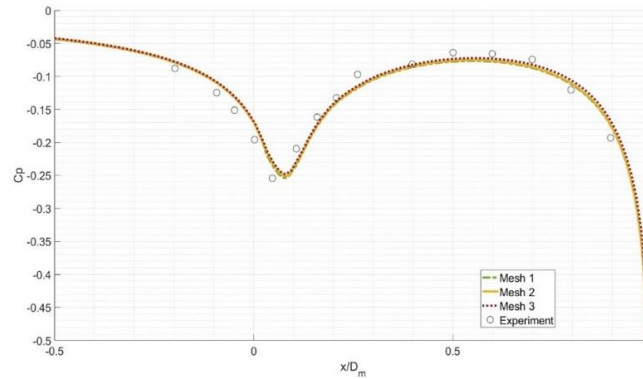
Figure 28 C_p profiles on the external surface and p_s/p_t profiles on the internal nozzle surface at NPR 4 and Mach number 1.2 ($D_m=15.24$ cm)

2.3.6 Grid Independency

There are 3 grids employed for 3D full geometry grid independency. Mesh details can be investigated by Table 7 Boattail and nozzle walls are refined and refined zones are created in nozzle region. Mesh 3 is used for analysis. Cp curves of employed grids are given in Figure 29.

Table 7 Grids for 3D Geometry

Mesh	Number of Elements
Mesh 1	7 120 470
Mesh 2	9 128 166
Mesh 3	13 739 125

Figure 29 Cp profiles on the external surface at an NPR 6 and Mach number of 0.9 ($D_m=15.24$ cm)

3. Conclusion

In this study, CFD analyses of an axisymmetric circular-arc boattail nozzle at transonic and supersonic freestream condition are investigated. Both open source (SU2) and commercial (ANSYS Fluent) CFD softwares are employed. Comparison with experiment is done via C_p and p_s/p_t with non dimensional x value (x/D_m). For SU2, Roe convective scheme with SST turbulence model is found to be more reliable with respect to other turbulence models and convective schemes employed in SU2 ;while, $k-\omega$ SST turbulence model of ANSYS Fluent is found more reliable with respect to other turbulence models employed in ANSYS Fluent.

References

- [1] G. T. Carson, Edwin. E. Lee. Experimental and Analytical Investigation of Axisymmetric Supersonic Cruise Nozzle Geometry at Mach Numbers from 0.6 to 1.3. NASA TP-1953, Hampton, Virginia, 1981.
- [2] Teryn DalBello, Nicholas. J. Georgiadis, Dennis. A. Yoder, Theo. G. Keith, "Computational Study of Axisymmetric Off-Design Nozzle Flows. In 42nd AIAA Aerospace Sciences Meeting and Exhibit, *Reno*, 2004
- [3] John. R. Carlson. Computational Prediction of Isolated Performance of an Axisymmetric Nozzle at Mach number 0.90. NASA Technical Memorandum 4506, Hampton, Virginia, 1994.
- [4] K. B. Bař and B. Çelik, "A Computational Investigation for Angle Of Attack Effect on Afterbody Drag," ITU, İstanbul, 2020.
- [5] F. D'Amico and D. A. Misul, "Turbulent Round Jet CFD Analysis with SU2 Code: from Validation to Aircraft's Exhaust," thesis, 2019.
- [6] F.R. Menter, "Zonal two equation $k-\omega$, turbulence models for aerodynamic flows," AIAA Paper 93-2906, 1993.